Title

The Chemokines CXCL9 and CXCL10 Promote a Protective Immune Response but Do Not Contribute to Cardiac Inflammation following Infection with Trypanosoma cruzi

Journal

Infection and Immunity, 74(1)

ISSN

0019-9567

Authors

Hardison, Jenny L
Wrightsman, Ruth A
Carpenter, Philip M
et al.

Publication Date

2006

DOI

10.1128/iai.74.1.125-134.2006

INFECTION AND IMMUNITY, Jan. 2006, p. 125–134 Vol. 74, No. 1
0019-9567/06/$08.00+0 doi:10.1128/IAI.74.1.125–134.2006

The Chemokines CXCL9 and CXCL10 Promote a Protective Immune Response but Do Not Contribute to Cardiac Inflammation following Infection with *Trypanosoma cruzi*

Jenny L. Hardison,[1] Ruth A. Wrightsman,[1] Philip M. Carpenter,[2] Thomas E. Lane,[1,3]* and Jerry E. Manning[1,3]

Department of Molecular Biology and Biochemistry[1] and Center for Immunology,[3] University of California, Irvine, California, and Department of Pathology and Laboratory Medicine, University of California at Irvine College of Medicine, Irvine, California[2]

Received 27 July 2005/Returned for modification 13 September 2005/Accepted 28 September 2005

The expression of chemokines within the heart during experimental infection of susceptible mice with the Colombiana strain of *Trypanosoma cruzi* was characterized in an attempt to determine a functional role for these molecules in both host defense and disease. Analysis of chemokine transcripts revealed that CXC chemokine ligand 9 (CXCL9) and CXCL10, as well as CC chemokine ligand 2 (CCL2) and CCL5, were prominently expressed during acute disease, whereas transcripts for CXCL9, CXCL10, and CCL5 remained elevated during chronic infection. Inflammatory macrophages present within the heart were the primary cellular source of these chemokines following *T. cruzi* infection. Peak chemokine expression levels coincided with increased gamma interferon expression and inflammation within the heart, suggesting a role for these molecules in both host defense and disease. Indeed, simultaneous treatment of *T. cruzi*-infected mice with neutralizing antibodies specific for CXCL9 and CXCL10 resulted in an increased parasite burden that was sustained out to 50 days p.i. Antibody targeting either CXCL10 or CCL5 did not change either *T. cruzi* burden within the heart nor attenuate the severity of cardiac inflammation at any time point examined, while targeting CXCL9 in combination with CXCL10 resulted in increased parasite burden. Collectively, these studies imply that CXCL9 and CXCL10 signaling enhances immune responses following parasite infection. However, antibody targeting of CXCL9 and CXCL10, or CXCL10 alone, or CCL5 alone does not directly modulate the inflammatory response within the heart, suggesting that other proinflammatory factors are able to regulate inflammation in this tissue in response to *T. cruzi* infection.

Chagas' disease is caused by infection with the protozoan parasite *Trypanosoma cruzi.* Currently there are 16 to 18 million people infected in Central and South America with 100 million at risk for infection (42). Approximately 20 to 30% of those infected will develop chronic cardiomyopathy 10 or 20 years after infection (4). Chagasic cardiomyopathy is characterized by inflammation and fibrosis of the heart, resulting in arrhythmias, thromboembolic events, dilated congestive cardiomyopathy, and eventual heart failure (28, 35). Inflammatory infiltrates in chronic Chagasic patients are composed of $CD4^+$ and $CD8^+$ T cells and macrophages, with $CD8^+$ T cells being the predominant cell type (15, 27). A protective immune response against *T. cruzi* is characterized by a T_H1-type response where the cytokines gamma interferon (IFN-γ), tumor necrosis factor alpha (TNF-α), and interleukin-12 (IL-12) play a crucial role in controlling infection (2, 30, 31, 38). Early in infection, molecules on the surface of *T. cruzi* stimulate the synthesis of IL-12 and TNF-α by macrophages (5). These cytokines stimulate the production of IFN-γ by different cell types, including NK cells, $CD4^+$ T cells, and $CD8^+$ T cells (2, 8). IFN-γ and TNF-α play a major role in resistance by activating macrophages to produce reactive nitrogen intermediates (6, 29–31) that are toxic to *T. cruzi* and function to control parasite replication (13, 16, 40). Infiltration of T cells and macrophages into the heart during acute infection is essential for controlling parasite replication in the heart as demonstrated by the increased cardiac parasitism in mice depleted of these cell types (23, 36). However, continued inflammation in the heart results in pathology characteristic of Chagas' disease.

The mechanisms underlying chronic infiltration of mononuclear cells into the heart years after infection with *T. cruzi* are largely unknown. However, studies have shown a positive correlation between the severity of infection during the acute phase of disease and the severity of cardiac disease seen in the chronic phase of disease (37). In addition, the presence of $CD8^+$ T cells in the hearts of Chagasic patients is correlated with the presence of parasite DNA and antigens, thus indicating that the parasite-stimulated immune response is likely responsible for chronic inflammation in the heart (15, 17).

There is currently no treatment available for treating chronic Chagas' disease. Understanding the mechanisms controlling infiltration of T cells and macrophages into the heart may identify potential therapeutic targets. Recent studies have focused on characterizing soluble factors that may initiate and/or amplify inflammation within the heart during *T. cruzi* infection. Gazzinelli and coworkers have determined there is an orchestrated chemokine expression profile within the heart following infection of susceptible mice with *T. cruzi* (34). Among the chemokines identified, the T-cell and macrophage chemoattractants CXC chemokine ligand 9 (CXCL9), CXCL10, and CC chemokine ligand 5 (CCL5) were expressed during both

* Corresponding author. Mailing address: Department of Molecular Biology and Biochemistry, 3205 McGaugh Hall, University of California at Irvine, Irvine, CA 92697-3900. Phone: (949) 824-5878. Fax: (949) 824-8551. E-mail: tlane@uci.edu.

acute and chronic disease, thus implicating these chemokines in initiating and maintaining chronic inflammation in the heart.

In the present study, we sought to characterize the expression of chemokines in the heart after infection with *T. cruzi* in an effort to elucidate their functional role in maintaining chronic inflammation. In addition, we also evaluated the expression of cytokines, as well as the level of inflammation and parasitism. Consistent with earlier studies (34), we report that chemokines CXCL9, CXCL10, and CCL5 are expressed in the heart during acute infection and these chemokines remain upregulated through chronic infection. Moreover, we demonstrate that macrophages are an early source of these chemokines within *T. cruzi*-infected cardiac tissue. In addition, the presence of these chemokine transcripts correlates with the expression of IFN-γ and TNF-α, as well as with the presence of inflammatory cells.

The abundant expression of CXCL9, CXCL10, and CCL5 during acute and chronic infection makes these molecules potentially relevant targets for neutralization to reduce cardiac inflammation associated with chronic *T. cruzi* infection. Therefore, *T. cruzi*-infected mice were treated either alone or combinations of neutralizing antibodies specific for CXCL9, CXC L10, and CCL5, and disease severity was evaluated. Treatment with a combination of both anti-CXCL9 and anti-CXCL10 resulted in increased parasitemia and cardiac parasitism, indicating a role for these chemokines in contributing to a protective immune response. However, our findings also indicate that ablation of signaling by these chemokines does not modulate the severity of inflammation at any time postinfection (p.i.) through day 60 p.i., suggesting that other proinflammatory factors are responsible for cardiac inflammation following *T. cruzi* infection.

MATERIALS AND METHODS

Mice. Female C56BL/6J mice were obtained from The Jackson Laboratory (Bar Harbor, ME) and used at 6 to 8 weeks of age.

Parasites and infection. The Colombiana strain (12) of *T. cruzi* was maintained as previously described by serial passage in female BALB/cByJ mice (43). Mice were infected subcutaneously with 50 blood-derived trypomastigotes. Animals were euthanized at various time points p.i., and hearts and spleens were collected for different assays.

Measurement of parasitemia. Parasitemia levels were determined as previously described (43) by removing a blood sample from the tail vein, diluting the sample in 0.9% ammonium chloride, and counting the trypomastigotes in a Neubauer hemacytometer (American Optical Corp., Buffalo, NY).

Cardiac tissue analysis. Hearts (three to six from each experimental group) were removed from mice at days 0, 15, 30, 60, 90, 120, and 200 p.i. and fixed in a 10% formalin solution. Hearts were then paraffin embedded, and 5-μm sections were cut at 100-μm increments. Sections used for inflammation scoring and analysis of infected cardiomyocytes were hematoxylin and eosin stained. Five sections from each heart were examined. Sectional areas were determined by scanning the slides into a digital image file, followed by measurement of the tissue area with the Scion Image analysis software package. Each section was scored blindly for inflammation with the system of Sun and Tarleton (32). To determine the degree of tissue parasitism, infected cardiomyocytes were counted in each hematoxylin-and-eosin-stained section. Infected cardiomyocytes have been estimated to be ca. 70 μm in diameter (26); thus, we have examined sections cut at 100-μm increments to reduce the probability of double counting the same infected cell.

Confocal microscopy. Hearts were removed from mice and frozen in O.C.T. media. Sections (8 μm) were cut by using a cryostat. Slides were desiccated overnight and fixed in acetone for 10 min at −20°C. Primary antibodies (diluted in phosphate-buffered saline containing 5% normal goat serum) used for dual fluorescent detection of cellular antigens were as follows: rat anti-mouse CD4, RM4-5 (BD Pharmingen, San Diego, CA) at 1:100; rat anti-mouse CD8b.2, Ly-3.2 (Pharmingen, San Diego, CA), at 1:100; rat anti-mouse F4/80 at 1:100 (SeroTec, Oxford, England); mouse anti-mouse CXCL9 at 1:20; mouse anti-mouse CXCL10 at 1:10; and mouse anti-mouse CCL5 at 1:20. An immunoglobulin G1 (IgG1) mouse anti-*Eimeria tenella* MAb was used as a negative control for chemokines staining (ATCC HB 8402). For detection of cell surface markers, primary antibodies to CD4, CD8, and F4/80 were used in combination with a fluorescein isothiocyanate-conjugated rat anti-mouse secondary antibody (Sigma, St. Louis, MO). For detection of chemokines, primary monoclonal antibodies (MAbs) to CXCL9 (derivation and characterization described below), CXCL10 (39), and CCL5 (14) were used in combination with a TRITC (tetramethyl rhodamine isothiocyanate)-conjugated rabbit anti-mouse secondary antibody (Sigma, St. Louis, MO). Dual-stained slides were then subjected to confocal microscopy using a Bio-Rad MRC UV laser-scanning confocal microscope (Bio-Rad, Richmond, CA).

RPA. Total RNA was extracted from hearts and spleens of mice collected on days 0, 15, 30, 60, and 120 p.i. by using TRIzol reagent (Invitrogen, Carlsbad, CA). A minimum of three mice per time point were assayed. Chemokine, chemokine receptor, cytokine, and cell surface marker transcripts were analyzed by using custom multitemplate probe sets (BD Pharmingen, San Diego, CA). RNase protection assay (RPA) analysis was performed with 12 μg of total RNA by a previously described protocol (20, 21). A probe for L32 was included to verify consistency in RNA loading and assay performance. For quantification of signal intensity, autoradiographs were scanned and transcript signals were normalized as the ratio of band intensity to the L32 control (20, 21). Analysis was performed by using Scion Image analysis software package.

Anti-CXCL9 MAb. A hybridoma cell line was created by immunizing BALB/c mice with peptides specific for CXCL9 (CISTSRGTIHYKSLK) coupled to keyhole lympet hemocyanin and fusing the spleens from these animals to SP2/0 myeloma with polyethylene glycol (3, 44). Hybridoma cell lines that produce antibody to this peptide were selected by sandwich enzyme-linked immunosorbent assay (ELISA) and recloned twice by limiting dilution. The target antigen for the ELISA was the same peptide used for immunization, but coupled to bovine serum albumin for maximal binding to the ELISA plates. This selection resulted in four clones specific for CXCL9. The final cell line utilized for all experiments reached a titer of >1:1,000,000 by ELISA using peptide as the target antigen. In addition, the final cell line was also selected based on MAb recognition of full-length CXCL9 protein by ELISA and viability in culture. The isotype of the anti-CXCL9 MAb was determined by using the IsoStrip kit (Roche Diagnostics, Indianapolis, IN). The clone selected (M11F8) was determined to be IgG2b κ. MAb was isolated from culture supernatants by affinity chromatography on Sepharose-protein G columns as previously described (44). Chemotaxis assays were performed by using transwell plates with a polycarbonate membrane (6.5-mm diameter, 5.0-μm pore size; Costar, Corning, NY). The ability of recombinant murine Mig (rMuMig; Biosource International, Camarillo, CA) to induce chemotaxis was assayed by using a cell line transfected with CXCR3 (300-19 cells, kindly provided by B. Moser). To determine whether anti-CXCL9 MAb blocked CXCL9 activity, chemotaxis assays were performed in Dulbecco modified Eagle medium supplemented with 25 mM HEPES buffer (pH 7.2), 1 mM sodium pyruvate, nonessential amino acids, L-glutamine, 5×10^{-5} M 2-mercaptoethanol, 50 U of penicillin/ml, 50 g of streptomycin sulfate, and 10% fetal bovine serum. Briefly, 400 ng of recombinant CXCL9 (Biosource International, Camarillo, CA)/ml was added to the lower transwell chamber with or without 200 μg of anti-CXCL9 MAb (M11F8)/ml in a total volume of 600 μl and preincubated at 37°C in 5% CO_2 for 30 min. Then, 5×10^5 $CXCR3^+$ cells were added to the upper chamber of the transwell in a total volume of 100 μl, and plates were incubated at 37°C in 5% CO_2 for 1.5 h. The contents of the lower well were removed, and cells counted by using a hemacytometer. The average of four quadrants counted in the hemacytometer was recorded and compared to cell migration to media alone. All assays were performed in duplicate.

Antibody treatment of mice. For all neutralization studies, mice were injected with 250 μg of each antibody intraperitoneally in a volume of 250 μl for neutralization of CXCL10 or CCL5 and 400 μl for neutralization of CXCL9 plus CXCL10 on the day of infection and every other day there after until euthanization. Isotype control antibodies were purified from culture supernatants of hybridoma cell lines S5B9 (IgG1, ATCC HB-8402; ATCC, Manassas, VA) and 5.2 (IgG2b, ATCC HB-9148). Control mice for studies neutralizing CXCL10 and CXCL9 plus CXLC10 were treated with 250 μg of IgG1 plus 250 μg of IgG2b in 400 μl per injection. Control mice for studies neutralizing CCL5 were treated with 250 μg of IgG2b in 250 μl per injection.

Statistical analysis. Data are expressed as means ± the standard deviation. Significant differences were determined by using the Student *t* test with *P* values of ≤0.05 being considered significant.

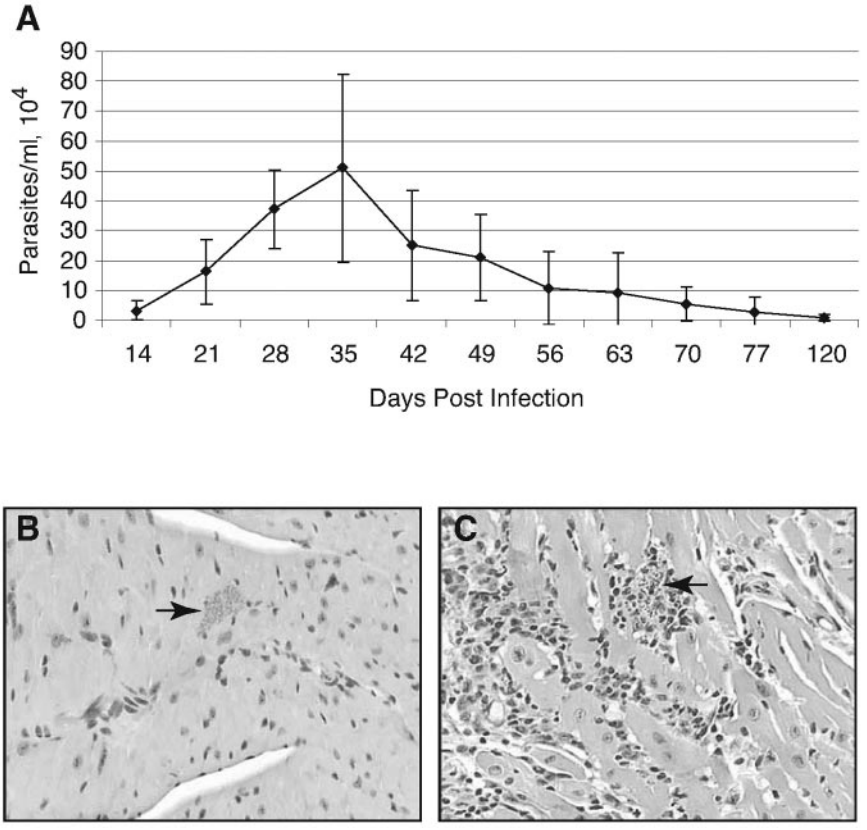

FIG. 1. C57BL/6 mice were infected with 50 trypomastigotes of the Colombiana strain of *T. cruzi*. Parasitemia was monitored weekly from days 12 to 77 p.i., and at day 120 p.i. for all mice infected; shown is the average parasitemia, in which a minimum of eight mice were counted per time point (A). Infected cells were observed in the heart at day 30 p.i., and amastigote nests are visible in hematoxylin and eosin stained sections as indicated by arrows occurring both in the absence of inflammation (B) and in the presence of inflammation (C).

RESULTS

Parasitemia and cardiac parasitism. C57BL/6 mice were infected with 50 parasites subcutaneously. Parasitemia was monitored weekly to monitor the course of infection. Parasitemia was detectable at day 14 p.i. and peaked at day 35 p.i. at 5.1×10^5 parasites/ml of blood (Fig. 1A). After day 35 p.i., parasitemia levels gradually decreased, and parasites were rarely detected during late chronic infection at day 120 p.i. Although mice developed significant parasitemia from infection, no mortality was observed through day 200 p.i. To assess cardiac tissue parasitism as well as evaluate the severity of inflammation, hearts were taken at days 0, 15, 30, 60, 90, 120, and 200 p.i. and stained with hematoxylin and eosin. Infected cardiomyocytes are easily detected as cells filled with darkly stained amastigotes at day 30 p.i. (Fig. 1B and C). Parasitized cardiomyocytes from five sections of each heart were quantified and expressed as the number of infected cells per 100 mm^2 of tissue. Cardiac parasitism was rarely detected at day 15 p.i. since only one infected cell was observed out of 10 hearts viewed (Fig. 1B). Correspondingly, inflammation into both the atrium and ventricle was relatively limited at this time (Table 1). Numerous infected cells were detected at day 30 p.i. in each sample viewed, with an average of 34.2 infected cells/100 mm^2 of tissue (Fig. 1B and C and Table 1). Correlating with the increase in parasite burden, cardiac inflammation peaked at day 30 p.i. but numerous inflammatory lesions were detectable out to 200 days p.i. (Table 1). Cardiac parasitism is mostly controlled by day 60 p.i., with only a few infected cells observed (Table 1), and parasitism is extremely rare at day 90 p.i. since only one infected cell was observed out of four samples viewed (data not shown). No infected cells were observed after day 90 p.i. Importantly, inflammation persists after the control of cardiac parasitism and parasitemia. Significant multifocal or diffuse inflammation is present in the heart at all time points observed after day 90 p.i. and out to day 200 p.i. (Table 1).

TABLE 1. Cardiac inflammation and tissue parasitism in C57BL/6 mice

Days p.i.	Avg inflammation score ± SD[a]		Tissue parasitism (no. of infected cells/100 mm^2) ± SE	*n*
	Atrium	Ventricle		
0	0.60 ± 0.55	0.67 ± 0.82	0.00	6
15	2.11 ± 0.33	2.00 ± 0.00	0.18 ± 0.57	10
30	4.00 ± 0.00	4.00 ± 0.00	34.20 ± 24.29	6
60	3.75 ± 0.50	3.50 ± 0.58	1.40 ± 1.81	4
90	3.25 ± 0.96	3.50 ± 0.58	0.31 ± 0.62	4
120	2.25 ± 0.50	2.00 ± 0.00	0.00	4
200	3.00 ± 0.00	3.67 ± 0.58	0.00	3

[a] Using the numerical scoring system of Sun and Tarleton (32).

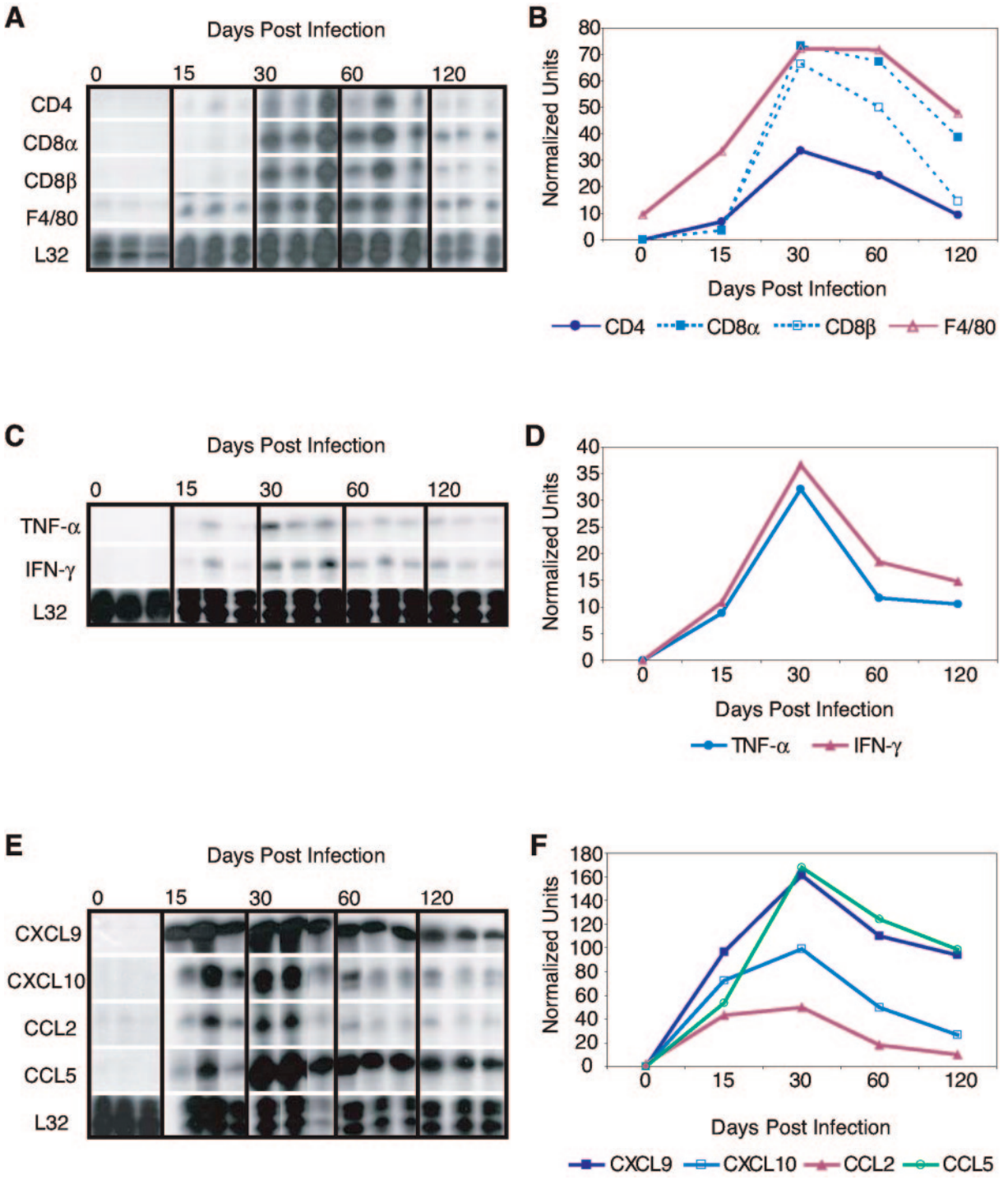

FIG. 2. Inflammatory cells and factors expressed within the heart were characterized by RPA at days 0, 15, 30, 60, and 120 p.i. Shown are representative RPA autoradiographs from three mice per time point (A, C, and E) and average quantitation of transcript expression normalized as a percentage of L32 expression (B, D, and F) for RPAs performed that assayed inflammatory cell marker expression (A and B), cytokine expression (C and D), and chemokine expression (E and F).

Characterization of inflammation in the heart. In order to obtain an overview of the cellular infiltrate present within the heart following *T. cruzi* infection, the presence of mRNA transcripts specific for unique cell surface markers was analyzed by RPA (Fig. 2A). This type of analysis reveals that markers for macrophages (F4/80) and T cells (CD4 and CD8) are expressed throughout infection but peak at day 30 p.i., and this correlates with peak inflammation as scored from cardiac tissue sections (Table 1 and Fig. 2B). Macrophages appear to be the dominant population of inflammatory cells at day 15 p.i.,

with transcript levels for F4/80 ~3-fold higher compared to uninfected mice. Expression of F4/80 peaks between 30 and 60 p.i. and diminishes modestly by day 120 p.i. (Fig. 2B). With regards to T-cell infiltration, transcripts associated with both $CD4^+$ and $CD8^+$ T cells are comparatively low at day 15 p.i. compared to F4/80 levels (Fig. 2A and B). By day 30 p.i., $CD8^+$ T-cell infiltration dramatically increases and slowly declines out to day 120 p.i. In contrast, CD4 transcripts are comparatively low at all time points examined compared to $CD8^+$ T-cell and macrophage-associated transcripts (Fig. 2B). Overall, these observations are consistent with earlier reports indicating that $CD8^+$ T cells and macrophages are relatively more numerous in cardiac inflammation compared to $CD4^+$ T cells (34).

Cytokine and chemokine expression in the heart. To assess the temporal expression of both cytokine and chemokines following *T. cruzi* infection, RPAs were used to quantitate the mRNA expression profiles within the heart at days 0, 15, 30, 60, and 120 p.i. Consistent with previous observations (5, 34, 36), cytokine expression in the heart is dominated by T_H1-associated cytokines, with transcripts for IFN-γ and TNF-α upregulated at day 15 p.i. and peaking at day 30 p.i. (Fig. 2C and D). Expression of CXCL9 and CXCL10, as well as CCL2 and CCL5, was detected in the heart at all time points after parasite infection (Fig. 2E and F). In general, the overall expression profile for each of these chemokines were similar to one another with detectable transcripts present within the heart at day 15 p.i. and peaked at day 30 p.i., followed by a gradual decline in transcript abundance. Transcripts for CXCL9 and CCL5 were relatively greater compared to CXCL10 and CCL2 at all time points examined (Fig. 2E and F). Overall, the expression kinetics of both cytokines and chemokines reached maximal expression, which coincided with maximal parasite burden and inflammation within the heart.

Macrophages express chemokines. To determine the cell types responsible for producing CXCL9, CXCL10, and CCL5 within the heart after infection with *T. cruzi*, confocal microscopy was performed on frozen heart sections staining for cell surface markers CD4, CD8, and F4/80 in combination with the chemokines listed above. Dual staining revealed that the primary source of chemokines at day 15 p.i. are macrophages (Fig. 3). The pattern of macrophage (F4/80) staining overlaps with the pattern of CXCL9 (Fig. 3A to C), CXCL10 (Fig. 3D to F), and CCL5 (Fig. 3G to I), indicating that macrophages are a source of these chemokines early following *T. cruzi* infection. Fewer T cells were observed in the heart at day 15 p.i. compared to macrophages and do not appear to be a major source of chemokine production at this time point (data not shown). In addition, examination of heart tissue at days 30, as well as 120 p.i. revealed an abundant presence of these chemokines throughout the heart, so much so that the precise cellular source could not be determined (data not shown).

Antibody targeting of chemokines. To investigate the functional contribution of chemokines CXCL9, CXCL10, and CCL5 to the control of parasitemia, parasite burden, and inflammatory cell infiltration into the heart of mice of mice infected with *T. cruzi*, MAbs that block the activity of these chemokines were used. Neutralizing antibodies specific for CXCL9, CXCL10 (9, 10, 39), or CCL5 (14) were administered to mice on the day of infection and every other day thereafter up to day 60 p.i. Infected mice were treated with either anti-CXCL10 or anti-CCL5 alone or a combination of anti-CXCL9 and anti-CXCL10. The rationale for simultaneous targeting of both CXCL10 and CXCL9 is due to the ability of these chemokines to bind the same receptor, CXCR3, thus eliminating the possibility of redundancy in signaling. Individual targeting of either CXCL10 (Fig. 4) or CCL5 (data not shown) had no effect on parasitemia. In contrast, when CXCL9 is neutralized in combination with CXCL10, parasitemia is significantly ($P \leq 0.05$) higher between days 21 to 49 p.i. compared to mice receiving isotype control MAbs (Fig. 4). These data suggest that CXCL9 may play some role, either solely or in combination with CXCL10, in controlling parasitemia.

To assess the effects of chemokine neutralization on parasitism and cardiac inflammation, hearts were removed from mice treated with neutralizing MAb(s) at days 15, 30, and 60 p.i. and stained with hematoxylin and eosin for quantitation of infected cells and scoring of inflammation. Neutralization of either CXCL10 or CCL5 alone did not result in increased cardiac parasitism compared to mice treated with isogenic control antibody (data not shown). Moreover, such treatment did not reduce cardiac inflammation in infected mice compared to control mice (data not shown). In contrast, simultaneous neutralization of CXCL10 and CXCL9 resulted in a significant increase ($P \leq 0.05$) in cardiac parasitism compared to mice treated with isotype control at day 30 p.i. (Table 2). At day 60 p.i. cardiac parasitism remains higher in antibody-treated mice compared to control treated mice, although this difference is not significant. However, blocking CXCL9 and CXCL10 does not prevent control of parasite replication during chronic disease at day 60 p.i. (Table 2), suggesting that control of parasitism is delayed in the absence of CXCL9 and CXCL10 signaling. Analysis of cardiac inflammation revealed no difference in the severity of inflammation in mice treated with anti-CXCL9 and anti-CXCL10 compared to control mice (Table 2). Consistent with these observations is the demonstration that ablation of CXCL9 and CXCL10 signaling did not alter transcript levels of inflammatory cell markers CD4, CD8, or F4/80 (Fig. 5A and B); cytokines TNF-α or IFN-γ (Fig. 5C and D); or chemokines CXCL9, CXCL10, or CCL5 (Fig. 5E and F) within the heart.

DISCUSSION

We used the Colombiana strain of *T. cruzi* to examine chemokine expression in the heart since this model results in disease in mice similar to that observed in natural human infection, namely: low parasitemia, intense cardiomyopathy, and cardiac parasitism that is controlled in the chronic phase of disease (12, 34). Murine infection with the Colombiana strain of *T. cruzi* results in relatively low level of parasitemia compared to infection with other strains (12), and parasitemia peaks at day 35 p.i. in agreement with previous studies using this model (34). Parasitemia is controlled during chronic infection and is rarely observed at day 120 p.i. (Fig. 1). Similarly, the development and increase in cardiac parasitism follows the same trend as parasitemia. Cardiac parasitism is scarce at day 15 p.i. but peaks at day 30 p.i. with numerous infected cells observed in all mice (Table 1). By day 60 p.i., replication is

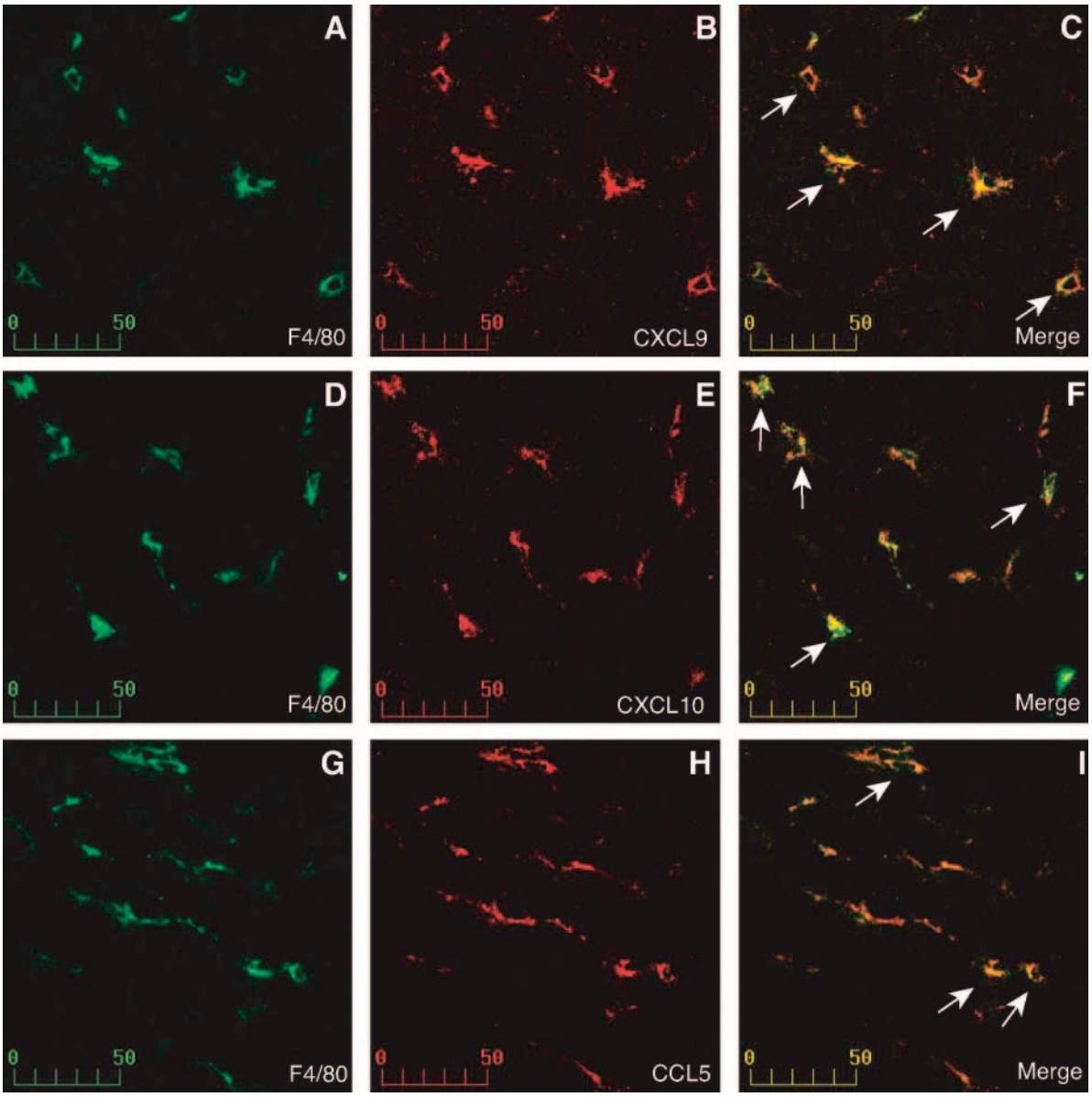

FIG. 3. Macrophages produce CXCL9, CXCL10, and CCL5 in the heart at day 15 p.i. Frozen sections from cardiac tissue taken at 15 days p.i. were stained with anti-F4/80 (green) (A, D, and G) and anti-CXCL9 (red), anti-CXCL10 (red), or anti-CCL5 (red). Shown are images of F4/80 alone (A, D, and G), chemokine alone (B, E, and H), and merged fluorescence (C, F, and I), with arrows indicating dual-positive cells.

controlled to low levels and parasites are not readily detected at day 120 p.i.

Expression of inflammatory cytokines and chemokines correlate with the presence of inflammatory cells within the heart. Consistent with previous observations (34), expression of markers for $CD4^+$ T cells, $CD8^+$ T cells, and macrophages are detected in the heart at day 15 p.i. and at peak levels at day 30 p.i. and remain highly expressed through day 120 p.i. (Fig. 2B). TNF-α and IFN-γ mRNA transcripts are expressed in the heart at day 15 p.i. (Fig. 2D). The level of cytokine expression increases >3-fold by day 30 and subsides at days 60 and 120 p.i., although expression never returns to basal levels, a finding consistent with continued inflammation. Chemokine transcripts are readily detected within the heart at day 15 p.i. with expression of CXCL9 > CXCL10 > CCL5 > CCL2 (Fig. 2F). Expression of chemokines also appeared to peak at day 30 p.i., with CXCL9 and CCL5 being the predominant chemokine transcripts detected. By day 120 p.i., limited transcript levels for the majority of chemokines are detected; however, CXCL9, CXCL10, and CCL5 transcript levels remain elevated. Further studies show that chemokine receptors CXCR3 and CCR5, which bind these chemokines (CXCL9 and CXCL10 and CCL5, respectively), are expressed in the hearts of mice infected with *T. cruzi* at similar times p.i. (14a). These data suggest that CXCL9, CXCL10, and CCL5 plays a role in maintaining chronic inflammation in the heart due to their continued high level of expression at day 120 p.i.

Confocal microscopy was used to identify the cellular source

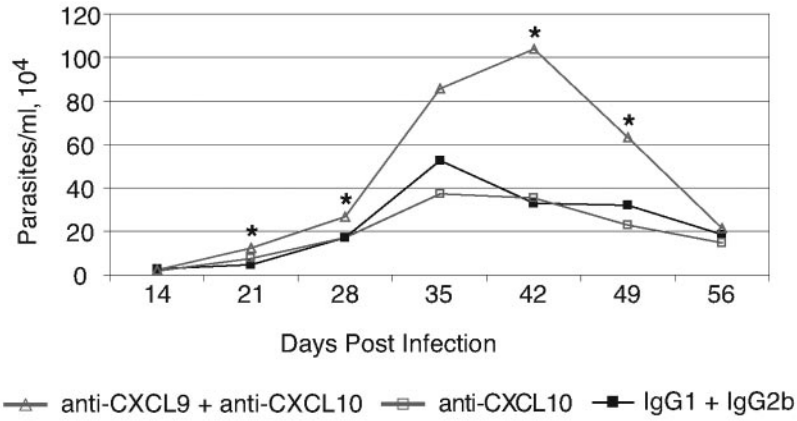

FIG. 4. Parasitemia is increased after neutralization of CXCL9 and CXCL10. Mice were treated with 250 μg of CXCL9 plus 250 μg of CXCL10 (△), 250 μg of CXCL10 (□), or 250 μg of IgG1 plus 250 μg of IgG2b isotype control (■). Parasitemia was monitored weekly beginning at day 14 p.i. Asterisks denote significant differences from the isotype control (Student *t* test, $P \leq 0.05$).

of chemokine expression in the heart in which we identified macrophages as a source of CXCL9, CXCL10, and CCL5 during acute infection (Fig. 3). The finding that macrophages are important sources of chemokines confirms an in vivo effector role for these cells (1, 7, 34). Numerous studies have characterized chemokine and cytokine production by macrophages cultured with either live trypomastigotes (2) or tGPI-mucins found on the surface of *T. cruzi* trypomastigotes (7, 11, 34). In addition, chemokines enhance effector functions of both human and mouse macrophages in vitro, suggesting that their production in vivo may also contribute to control of parasite replication by mechanisms other than recruitment of lymphocytes (1, 22, 41). Thus, macrophages are an important source of chemokines early in *T. cruzi* infection and likely contribute to the establishment and maintenance of cardiac inflammation. Studies in other models also show that macrophages are an important source of chemokines in vivo. For example, Zhao et al. demonstrated that macrophages express various chemokines including CXCL9 and CXCL10 in a mouse model for heart transplant rejection (46). These observations support our conclusion that macrophages are important sources of chemokines in the heart following *T. cruzi* infection.

Characterization of chemokine expression within the heart suggests that CXCL9, CXCL10, and CCL5 may be involved in mechanisms initiating and maintaining chronic inflammation in the heart. We sought to dissect the role of these chemokines in cardiac inflammation by neutralizing CXCL10 and CCL5 alone or CXCL9 in combination with CXCL10 by using MAbs specific for each chemokine. Surprisingly, none of the chemokine neutralization strategies used in the present study resulted in amelioration of cardiac inflammation from days 15 to 60 p.i. (Table 2). In addition, neutralization of a single chemokine (CXCL10 or CCL5) did not result in any pronounced lapse in host defense or reduction of inflammation, as has been reported in other models (18, 45). This difference may be due to the kinetics of chemokine expression since CXCL9, CXCL10, and CCL5 are all upregulated as early as day 10 p.i. (data not shown), whereas in other infections such as *T. gondii* (18) only CXCL10 is prominently expressed early in infection before other chemokines are upregulated. Neutralization of CXCL9 in combination with CXCL10 resulted in a marked reduction in the ability of the host to control parasite replication within both the blood and the heart. After neutralization of CXCL9 and CXCL10, parasitemia was higher from days 21 to 49 p.i. combined with an ~2-fold increase in cardiac parasitism at day 30 p.i. (Fig. 4 and Table 2). Thus, CXCL9 or the combination of CXCL9 and CXCL10 is needed for an efficient protective host response to *T. cruzi* infection.

TABLE 2. Cardiac inflammation and tissue parasitism following chemokine neutralization

Antibody treatment	Days p.i.	Avg inflammation score ± SD[a]		Tissue parasitism (no. of infected cells/100 mm^2) ± SE
		Atrium	Ventricle	
IgG1 + IgG2b	15	2.00 ± 1.00	1.67 ± 0.58	1.59 ± 1.43
	30	4.00 ± 0.00	3.67 ± 0.58	15.70 ± 6.30
	60	4.00 ± 0.00	4.00 ± 0.00	0.86 ± 1.50
Anti-CXCL9 + anti-CXCL10	15	2.00 ± 0.00	2.00 ± 0.00	0.00 ± 0.00
	30	4.00 ± 0.00	4.00 ± 0.00	33.59 ± 13.75[b]
	60	4.00 ± 0.00	3.67 ± 0.58	3.57 ± 5.00

[a] Using the numerical scoring system of Sun and Tarleton (32).
[b] Significantly different from isotype control (Student's *t* test, $P \leq 0.05$). Data represent three mice per group per time point.

A number of mechanisms contribute to the control of parasite replication during *T. cruzi* infection. Select depletion of T-cell subsets or macrophages during *T. cruzi* infection results in increased parasitemia and tissue parasite burden, thus illustrating the important role these cells play in controlling parasite replication (23, 36). One mechanism by which $CD4^+$ and $CD8^+$ T cells contribute to the control of parasite replication is through the production IFN-γ early in infection. IFN-γ activates infected macrophages to upregulate iNOS, resulting in the production of reactive nitrogen intermediates that are directly toxic to *T. cruzi* (16, 40). Activated macrophages will also increase phagocytosis of trypomastigotes, thus providing a mechanism for clearing extracellular trypomastigotes. In addition, cytotoxic activity by $CD8^+$ T cells also contributes to control of tissue parasitism and parasitemia, since mice defi-

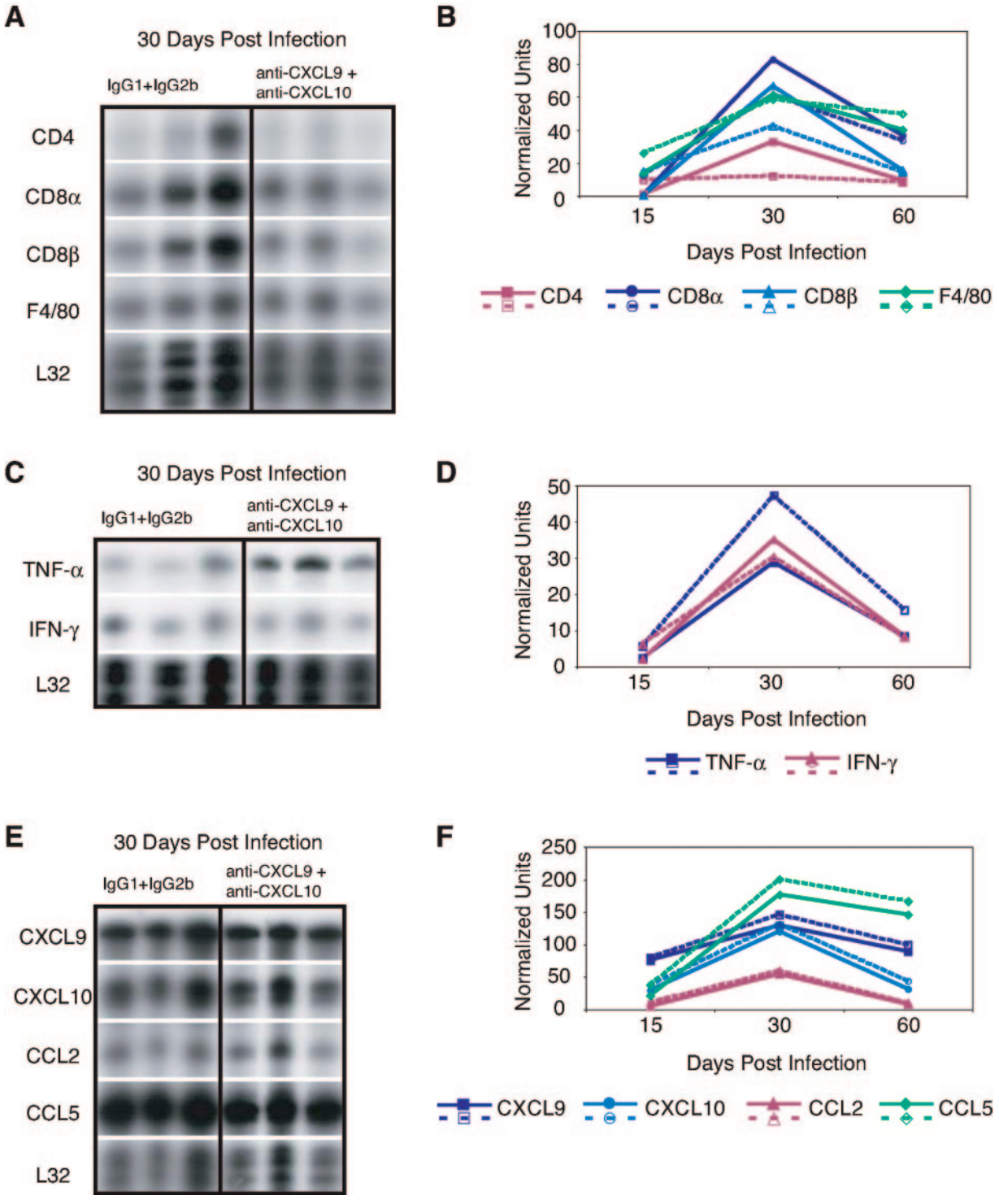

FIG. 5. Inflammatory cells and factors expressed within the heart were characterized by RPA at days 15, 30, and 60 in mice treated with isotype control antibody or anti-CXCL9 plus anti-CXCL10 MAb. Shown are representative RPA autoradiographs from samples at day 30 p.i. and average quantitation of transcript expression normalized as a percentage of L32 expression (B, D, and F) for RPAs performed that assayed inflammatory cell marker expression (A and B), cytokine expression (C and D), and chemokine expression (E and F).

cient in perforin and granzyme had increased parasitemia, tissue parasite burden, and early mortality (24).

The mechanism by which combined anti-CXCL9 and anti-CXCL10 treatment contributes to protective host immunity is not entirely clear since infiltration of $CD4^+$ and $CD8^+$ T cells and macrophages into the heart was not significantly reduced at day 30 p.i, and expression of IFN-γ and TNF-α was unchanged (Fig. 5). Perhaps, the activation of infiltrating T cells

is adversely affected in the absence of CXCL9 and CXCL10 signaling, resulting in a muted effector function. Reduced cytotoxic-T-lymphocyte activity could explain increased tissue parasitism seen following neutralization of CXCL9 and CXCL10 since other studies neutralizing CXCL10 reported decreased $CD8^+$-T-cell-mediated killing and antigen-specific cell-mediated immunity (18). However, complete effector functions are likely attained later in infection or compensatory mechanisms engaged, since cardiac parasitism is greatly reduced by day 60 p.i., a finding consistent with the production of IFN-γ and TNF-α. Lastly, reduction of parasitemia to control levels by day 56 p.i. is likely a result of circulating antibody.

The present study confirms previous reports that dominant chemokines expressed during both acute and chronic *T. cruzi* infection are CXCL9, CXCL10, and CCL5. Further, we show that macrophages are an important in vivo source of each of these chemokines early after infection, thus expanding the role of macrophages in initiating inflammation in the heart during *T. cruzi* infection. Antibody neutralization of CXCL10, CCL5, or CXCL9 in combination with CXCL10 revealed a role for CXCL9 in conjunction with CXCL10 in controlling parasite replication. To our surprise, however, these chemokine neutralization strategies did not alleviate cardiac inflammation. Therefore, further studies are needed to define chemokine-chemokine receptor interactions essential for maintaining cardiac inflammation during chronic *T. cruzi* infection.

ACKNOWLEDGMENTS

This study was supported by National Institutes of Health grants AI18873 (J.E.M.) and NS41249 and NS18146 (T.E.L.). J.L.H. is supported by postdoctoral fellowship 1562-A-1 from the National Multiple Sclerosis Society.

REFERENCES

1. **Aliberti, J. C., F. S. Machado, J. T. Souto, A. P. Campanelli, M. M. Teixeira, R. T. Gazzinelli, and J. S. Silva.** 1999. β-Chemokines enhance parasite uptake and promote nitric oxide-dependent microbiostatic activity in murine inflammatory macrophages infected with *Trypanosoma cruzi*. Infect. Immun. **67:**4819–4826.
2. **Aliberti, J. C. S., M. A. G. Cardoso, G. A. Martins, R. T. Gazzinelli, L. Q. Vieira, and J. S. Silva.** 1996. Interleukin-12 mediates resistance to *Trypanosoma cruzi* in mice and is produced by murine macrophages in response to live trypomastigotes. Infect. Immun. **64:**1961–1967.
3. **Beard, C. A., R. A. Wrightsman, and J. E. Manning.** 1988. Stage and strain specific expression of the tandemly repeated 90 kDa surface antigen gene family in *Trypanosoma cruzi*. Mol. Biochem. Parasitol. **28:**227–234.
4. **Brener, Z.** 1992. Chagas disease—clinical features: Chagas disease (American trypanosomiasis): its impact on transfusion and clinical medicine. Int. Soc. Blood Trans. Cap. **6:**81–101.
5. **Camargo, M. M., I. C. Almeida, M. E. Pereira, M. A. Ferguson, L. R. Travassos, and R. T. Gazzinelli.** 1997. Glycosylphosphatidylinositol-anchored mucin-like glycoproteins isolated from *Trypanosoma cruzi* trypomastigotes initiate the synthesis of proinflammatory cytokines by macrophages. J. Immunol. **158:**5890–5901.
6. **Camargo, M. M., A. C. Andrade, I. C. Almeida, L. R. Travassos, and R. T. Gazzinelli.** 1997. Glycoconjugates isolated from *Trypanosoma cruzi* but not from Leishmania species membranes trigger nitric oxide synthesis as well as microbicidal activity in IFN-γ-primed macrophages. J. Immunol. **159:**6131–6139.
7. **Campos, M. A., I. C. Almeida, O. Takeuchi, S. Akira, E. P. Valente, D. O. Procopio, L. R. Travassos, J. A. Smith, D. T. Golenbock, and R. T. Gazzinelli.** 2001. Activation of Toll-like receptor-2 by glycosylphosphatidylinositol anchors from a protozoan parasite. J. Immunol. **167:**416–423.
8. **Cardillo, F., J. C. Voltarelli, S. G. Reed, and J. S. Silva.** 1996. Regulation of *Trypanosoma cruzi* infection in mice by gamma interferon and interleukin 10: role of NK cells. Infect. Immun. **64:**128–134.
9. **Carr, D. J., J. Chodosh, J. Ash, and T. E. Lane.** 2003. Effect of anti-CXCL10 monoclonal antibody on herpes simplex virus type 1 keratitis and retinal infection. J. Virol. **77:**10037–10046.
10. **Cliffe, L. J., N. E. Humphreys, T. E. Lane, C. S. Potten, C. Booth, and R. K. Grencis.** 2005. Accelerated intestinal epithelial cell turnover: a new mechanism of parasite expulsion. Science **308:**1463–1465.
11. **Coelho, P. S., A. Klein, A. Talvani, S. F. Coutinho, O. Takeuchi, S. Akira, J. S. Silva, H. Canizzaro, R. T. Gazzinelli, and M. M. Teixeira.** 2002. Glycosylphosphatidylinositol-anchored mucin-like glycoproteins isolated from *Trypanosoma cruzi* trypomastigotes induce in vivo leukocyte recruitment dependent on MCP-1 production by IFN-gamma-primed-macrophages. J. Leukoc. Biol. **71:**837–844.
12. **Federici, E. E., W. H. Albemann, and F. A. Neva.** 1964. Chronic and progressive myocarditis and myositis in C3H mice infected with *Trypanosoma cruzi*. Am. J. Trop. Med. Hyg. **13:**272–280.
13. **Gazzinelli, R. T., I. P. Oswald, S. Hieny, S. L. James, and A. Sher.** 1992. The microbicidal activity of interferon-gamma-treated macrophages against *Trypanosoma cruzi* involves an L-arginine-dependent, nitrogen oxide-mediated mechanism inhibitable by interleukin-10 and transforming growth factor-β. Eur. J. Immunol. **22:**2501–2506.
14. **Glass, W. G., M. J. Hickey, J. L. Hardison, M. T. Liu, J. E. Manning, and T. E. Lane.** 2004. Antibody targeting of the CC chemokine ligand 5 results in diminished leukocyte infiltration into the central nervous system and reduced neurologic disease in a viral model of multiple sclerosis. J. Immunol. **172:**4018–4025.

14a. **Hardison, J. L., R. A. Wrightsman, P. M. Carpenter, W. A. Kuziel, T. E. Lane, and J. E. Manning.** The CC chemokine receptor 5 is important in control of parasite replication and acute cardiac inflammation following infection with *Trypanosoma cruzi.* Infect. Immun. **74:**135–143.

15. **Higuchi, M. D., M. M. Ries, V. D. Aiello, L. A. Benvenuti, P. S. Gutierrez, G. Bellotti, and F. Pileggi.** 1997. Association of an increase in $CD8^+$ T cells with the presence of *Trypanosoma cruzi* antigens in chronic, human, chagasic myocarditis. Am. J. Trop. Med. Hyg. **56:**485–489.
16. **Holscher, C., G. Kohler, U. Muller, H. Mossmann, G. Schaub, and F. Brombacher.** 1998. Defective nitric oxide effector functions lead to extreme susceptibility of *Trypanosoma cruzi*-infected mice deficient in gamma interferon receptor or inducible nitric oxide synthase. Infect. Immun. **66:**1208–1215.
17. **Jones, E. M., D. G. Colley, S. Tostes, E. R. Lopes, C. L. Vnencak-Jones, and T. L. McCurley.** 1993. Amplification of a *Trypanosoma cruzi* DNA sequence from inflammatory lesions in human chagasic cardiomyopathy. Am. J. Trop. Med. Hyg. **48:**348–357.
18. **Kahn, I. A., J. A. MacLean, F. S. Lee, L. Casciotti, E. DeHaan, J. D. Schwartzman, and A. D. Luster.** 2000. IP-10 is critical for effector T-cell trafficking and host survival in *Toxoplasma gondii* infection. Immunity **12:**483–494.
19. Reference deleted.
20. **Lane, T. E., V. C. Asensio, N. Yu, A. D. Paoletti, I. L. Campbell, and M. J. Buchmeier.** 1998. Dynamic regulation of alpha and beta chemokine expression in the central nervous system during mouse hepatitis virus-induced demyelinating disease. J. Immunol. **160:**970–978.
21. **Lane, T. E., M. T. Liu, B. P. Chen, V. C. Asensio, R. M. Samawi, A. L. Paoletti, I. L. Campbell, S. L. Kunkel, H. S. Fox, and M. J. Buchmeier.** 2000. A central role for $CD4^+$ T cells and RANTES in virus-induced central nervous system inflammation and demyelination. J. Virol. **74:**1415–1424.
22. **Lima, M. F., Y. Zhang, and F. Villalta.** 1997. Beta-chemokines that inhibit HIV-1 infection of human macrophages stimulate uptake and promote destruction of *Trypanosoma cruzi* by human macrophages. Cell Mol. Biol. **43:**1067–1076.
23. **Melo, R. C., and C. R. Machado.** 2001. *Trypanosoma cruzi*: peripheral blood monocytes and heart macrophages in the resistance to acute experimental infection in rats. Exp. Parasitol. **97:**15–23.
24. **Muller, U., V. Sobek, S. Balkow, C. Holscher, A. Mullbacher, C. Museteanu, H. Mossmann, and M. M. Simon.** 2003. Concerted action of perforin and granzymes is critical for the elimination of *Trypanosoma cruzi* from mouse tissues, but prevention of early host death is in addition dependent on the FasL/Fas pathway. Eur. J. Immunol. **33:**70–78.
25. Reference deleted.
26. **Postan, M., J. A. Dvorak, and J. P. McDaniel.** 1983. Studies of *Trypanosoma cruzi* clones in inbred mice. I. A comparison of the course of infection of C3H/HEN− mice with two clones isolated from a common source. Am. J. Trop. Med. Hyg. **32:**497–506.
27. **Reis, D. D., E. M. Jones, S. Tostes, E. R. Lopes, G. Gazzinelli, D. G. Colley, and T. L. McCurley.** 1993. Characterization of inflammatory infiltrates in chronic chagasic myocardial lesions: presence of tumor necrosis factor-α^+ cells and dominance of granzyme A^+, $CD8^+$ lymphocytes. Am. J. Trop. Med. Hyg. **48:**637–644.
28. **Rossi, M. A., and R. B. Bestetti.** 1995. The challenge of chagasic cardiomyopathy. Cardiology **86:**1.
29. **Silva, J. S., J. C. Aliberti, G. A. Martins, M. A. Souza, J. T. Souto, and M. A. Padua.** 1998. The role of IL-12 in experimental *Trypanosoma cruzi* infection. Braz. J. Med. Biol. Res. **31:**111–115.
30. **Silva, J. S., P. J. Morrissey, K. H. Grabstein, K. M. Mohler, D. Anderson, and S. G. Reed.** 1992. Interleukin 10 and interferon gamma regulation of experimental *Trypanosoma cruzi* infection. J. Exp. Med. **175:**169–174.
31. **Silva, J. S., G. N. Vespa, M. A. Cardoso, J. C. Aliberti, and F. Q. Cunha.**

1995. Tumor necrosis factor alpha mediates resistance to *Trypanosoma cruzi* infection in mice by inducing nitric oxide production in infected gamma interferon-activated macrophages. Infect. Immun. **63:**4862–4867.
32. **Sun, J., and R. L. Tarleton.** 1993. Predominance of $CD8^+$ T lymphocytes in the inflammatory lesions of mice with acute *Trypanosoma cruzi* infection. Am. J. Trop. Med. Hyg. **48:**161–169.
33. Reference deleted.
34. **Talvani, A., C. S. Ribeiro, J. C. Aliberti, V. Michailowsky, P. V. Santos, S. M. Murta, A. J. Romanha, I. C. Almeida, J. Farber, J. Lannes-Vieira, J. S. Silva, and R. T. Gazzinelli.** 2000. Kinetics of cytokine gene expression in experimental chagasic cardiomyopathy: tissue parasitism and endogenous IFN-gamma as important determinants of chemokine mRNA expression during infection with *Trypanosoma cruzi*. Microbes Infect. **2:**851–866.
35. **Tanowitz, H. B., L. V. Kirchhoff, F. Simon, S. A. Morris, L. M. Weiss, and M. Wittner.** 1992. Chagas disease. Clin. Microbiol. Rev. **5:**400–419.
36. **Tarleton, R. L., J. Sun, L. Zhang, and M. Postan.** 1994. Depletion of T-cell subpopulations results in exacerbation of myocarditis and parasitism in experimental Chagas' disease. Infect. Immun. **62:**1820–1829.
37. **Teixeira, A. R., P. S. Monteiro, J. M. Rebelo, E. R. Arganaraz, D. Vieira, L. Lauria-Pires, R. Nascimento, C. A. Vexenat, A. R. Silva, S. K. Ault, and J. M. Costa.** 2001. Emerging Chagas disease: trophic network and cycle of transmission of *Trypanosoma cruzi* from palm trees in the Amazon. Emerg. Infect. Dis. **7:**100–112.
38. **Torrico, F., H. Heremans, M. T. Rivera, E. Van Marck, A. Billiau, and Y. Carlier.** 1991. Endogenous IFN-gamma is required for resistance to acute *Trypanosoma cruzi* infection in mice. J. Immunol. **146:**3626–3632.
39. **Trifilo, M. J., C. Montalto-Morrison, L. N. Stiles, K. R. Hurst, J. L. Hardison, J. E. Manning, P. S. Masters, and T. E. Lane.** 2004. CXC chemokine ligand 10 controls viral infection in the central nervous system: evidence for a role in innate immune response through recruitment and activation of natural killer cells. J. Virol. **78:**585–594.
40. **Vespa, G. N., F. Q. Cunha, and J. S. Silva.** 1994. Nitric oxide is involved in control of *Trypanosoma cruzi*-induced parasitemia and directly kills the parasite in vitro. Infect. Immun. **62:**5177–5182.
41. **Villalta, F., Y. Zhang, K. E. Bibb, J. C. Kappes, and M. F. Lima.** 1998. The cysteine-cysteine family of chemokines RANTES, MIP-1α, and MIP-1β induce trypanocidal activity in human macrophages via nitric oxide. Infect. Immun. **66:**4690–4695.
42. **World Health Organization.** 1991. Control of Chagas' disease. W. H. O. Tech. Ser. **811:**1–93.
43. **Wrightsman, R., S. Krassner, and J. Watson.** 1982. Genetic control of responses to *Trypanosoma cruzi* in mice: multiple genes influencing parasitemia and survival. Infect. Immun. **36:**637–644.
44. **Wrightsman, R. A., W. Leon, and J. E. Manning.** 1986. Variation in antigenic determinants specific to the infective stage of *Trypanosoma cruzi*. Infect. Immun. **53:**235–239.
45. **Yun, J. J., M. P. Fischbein, D. Whiting, Y. Irie, M. C. Fishbein, M. Burdick, D., J. Belperio, R. M. Strieter, H. Laks, J. A. Berliner, and A. Ardehali.** 2002. The role of MIG/CXCL9 in cardiac allograft vasculopathy. Am. J. Pathol. **161:**1307–1313.
46. **Zhao, D. X., Y. Hu, G. G. Miller, A. D. Luster, R. N. Mitchell, and P. Libby.** 2002. Differential expression of the IFN-gamma-inducible CXCR3-binding chemokines, IFN-inducible protein 10, monokine induced by IFN, and IFN-inducible T-cell alpha chemoattractant in human cardiac allografts: association with cardiac allograft vasculopathy and acute rejection. J. Immunol. **169:**1556–1560.

Editor: W. A. Petri, Jr.